Carbohydrate Polymers 86 (2011) 296–303

Contents lists available at ScienceDirect

Carbohydrate Polymers

journal homepage: www.elsevier.com/locate/carbpol

Grafting of 4-aminoantipyrine from guar gum substrates using graft atom transfer radical polymerization (ATRP) process

Vivek Mishra, Rajesh Kumar*

Organic Polymer Laboratory, Department of Chemistry, Centre of Advance Studies in Chemistry, Faculty of Science, Banaras Hindu University, Varanasi 221005, UP, India

ARTICLE INFO

Article history:
Received 3 November 2010
Received in revised form 18 April 2011
Accepted 20 April 2011
Available online 6 May 2011

Keywords:
ATRP graft copolymer
4-Aminoantipyrine
Guar gum
Thermal analysis

ABSTRACT

ATRP graft copolymerization of 4-aminoantipyrine (AAP) was carried out successfully at 50 °C from a guar gum based macroinitiator (GGBr), Cu(I)Br and 2,2′-bipyridyl(bpy) as initiator, catalyst and ligand, respectively, in water. Factors affecting the conversion and rate of graft copolymerization such as temperature, concentration of monomer, catalyst, ligand and initiator were studied. The best initial molar concentration ratio of [AAP]:[GGBr]:[Cu(I)Br]:[bpy] was found 100:1:1:2 for controlled graft copolymerization. The plot $\ln[M]_0/[M]_t$ vs. time showed first order kinetics with respect to 4-aminoantipyrine. The activation energy (E_a = 25.15 kJ mol^{-1}), enthalpy of activation ($\Delta H^{\ddagger}$ = 22.42 kJ mol^{-1}) and negative value of entropy of transition state ($\Delta S^{\ddagger}$ = −233.82 J mol^{-1} K^{-1}) support the progress of polymerization reaction. The % grafting ratio was found to be 5184% and the graft copolymer was characterised by ^{1}H NMR, FTIR, UV, GPC, XRD, TGA and DSC analyses.

1. Introduction

Pyrazolone is an active moiety as a pharmaceutical ingredient, especially in non-steroidal anti-inflammatory drugs (NSAID) and is used in the treatment of arthritis and other musculoskeletal and joint disorders. Antipyrine was used as an antipyretic, but replaced due to the possibility of agranulocytosis side effect. Lactam is in demand in the artificial fibre industry. Pyrazolone derivatives, which have a related structure to lactam are also widely used in preparing dyes and pigments. Pyrazolines are five-membered nitrogen containing heterocyclic compounds. Formation of pyrazoline was reported (Desai, Modi, & Naik, 1994; Kadu & Jamode, 1998; Raman, Kulandaisamy, Shunmugasundaram, & Jeyasubramanian, 2001; Samath, Jeyasubramanian, Thambidurai, Kamardeen, & Ramalingam, 1993; Utale, Raghuvanshi, & Doshi 1998) by the action of nucleophiles like hydrazine hydrate or phenyl hydrazine etc. Pyrazolines are used in textiles as fungicidal (Sachchar & Singh, 1985), analgesic (Metwally, Yousif, Ismaiel, & Amer, 1985) and antimicrobial agents (Kadu, Jamode, Tambekar 1999; Tayde & Jamode, 1998).

Polysaccharides have been the subject of much research attention due to their sustainability, biodegradability and scale of production (Beers, Gaynor, Matyjaszewski, Sheiko, & Moeller, 1998; Kamigaito, Ando & Sawamoto 2001). Modification of these natural materials by graft copolymerization and atom transfer radical polymerization using hetero-aromatic monomers offer the opportunity to tailor their physical and chemical properties, yielding functional macromolecules that may find a wide range of applications (Matyjaszewski & Xia, 2001; Wang & Matyjaszewski, 1995; Wang, Lascelles, Jackson, & Armes, 1999). The beauty of ATRP is that it allows great control over the molecular weight distribution and the architecture of polymers. Moreover, it is very tolerant of a variety of functional groups and protic solvents, including water (Kamigaito et al., 2001; Matyjaszewski & Xia, 2001). An advantage of this synthetic method is the defined nature of the side chain distribution (Ebouc, Dez, Desbrieres, Picton, & Madec, 2005; Gorochovceva & Makuska, 2004; Huang, Shen, & Fang 2005; Kurita, Amemiya, Mori, & Nishiyama, 1999; Mishra & Kumar, 2011; Roos, Muller, & Matyjaszewski, 2000; Shinoda & Matyjaszewski, 2001; Shinoda, Miller, & Matyjaszewski, 2001) and the control of the main chain parameters, degree of polymerization (DP_n) and molar mass distribution.

One of the major difficulties in preparing pure graft copolymer is the formation of homopolymers by conventional free radical polymerization (Banerjee, Kumar, Srivastava, & Behari, 2006; Behari, Kumar, Tripathi, & Pandey, 2001a; Behari, Pandey, Kumar, & Taunk, 2001b; Kumar, Srivastava, & Behari, 2009; Srivastava, Mishra, Singh, & Kumar, 2010), which are difficult to remove (Jenkins & Hudson, 2001; Kumar, Srivastava, & Behari, 2007, 2008; Srivastava, Mishra, Singh, & Kumar, 2009; Tripathi, Behari, Taunk, & Kumar, 2000) from the graft copolymer network. The problems with conventional free radical polymerization, applications of 4-aminoantipyrine, and hitherto unreported graft copolymerization

* Corresponding author. Tel.: +91 5426702501; fax: +91 5422368174.
E-mail addresses: vivek_bhuchem@yahoo.co.in (V. Mishra), rkr_bhu@yahoo.com (R. Kumar).

0144-8617/$ – see front matter © 2011 Elsevier Ltd. All rights reserved.
doi:10.1016/j.carbpol.2011.04.052

of guar gum via the ATRP process using the "from" technique of grafting prompted us to develop an approach to overcome the problems, and thus we designed graft copolymerization via the ATRP process of 4-aminoantipyrine from guar gum as a macro initiator, which gives a controlled molar mass distribution, functionalities with high % of grafting and without formation of a homopolymer by-product. Such modification substantially changes the reactivity and activity of the polymers and makes guar gum and 4-aminoantipyrine more potent and functional.

2. Experimental

2.1. Materials

Tetrahydrofuran (THF) (Merck) was dried using sodium and benzophenone and refluxed for 8 h then distilled out and used at once. Dimethyl sulfoxide (Merck) was refluxed over CaH_2 and distilled under reduced pressure. Chloroform (Merck) was shaken with several portions of concentrated H_2SO_4 (Merck), washed thoroughly with water, and dried with $CaCl_2$ before it was filtered and distilled. 4-aminoantipyrine, Guar gum, 2-bromo isobutyroic acid, carbonyl diimidazole, LiCl was used as received from Aldrich. Cu (I)Br (99%, Aldrich) was purified by six times washing with glacial acetic acid (Merck) and three times with anhydrous ethanol (Merck). They were dried under vacuum at room temperature and stored under nitrogen atmosphere. 2,2′-bipyridine (bpy) was purchased from Aldrich and was recrystallised from ethanol to remove impurities. Basic aluminium oxide (Himedia, India) was activated in oven before use.

2.2. Instrumental analyses

^1H NMR analysis: ^1H NMR was recorded on a JEOL AL300 FT-NMR spectrophotometer in $CDCl_3$ and D_2O containing TMS as the internal standard, Signals are quoted in parts per million (δ ppm) relative to TMS.

FTIR analysis: The FTIR spectra recorded by from pellets in KBr (AR grade) containing 51% sample, using a Varian Excalibur 3000 model.

UV analysis: The UV spectra of guar gum, guar gum macro initiator and guar gum-g-(4-aminoantipyrine) was recorded in water on PerkinElmer–Lambda 35 UV–vis Spectrophotometer at 25 °C using PTP 1 (Peltier Temperature programmer). The optical path length of measurement cell was 10 mm and concentration of the solution was 0.1% (w/v).

The electronic absorption spectra of guar gum, guar gum macroinitiator, 4-aminoantipyrine and GGBr-g-AAP were taken in water in the 200–400 nm region.

GPC analysis: The number and weight-average molecular weights (Mn and Mw, respectively) of the synthesised graft copolymers were measured by GPC comprised of a Waters SEC equipped with two 300-mm Waters Styragel solvent-saving columns (molecular weight ranges: 5×10^2–3×10^4; 5×10^3–6×10^5) and a Waters 2414 refractive index detector. The eluent was THF at a flow rate of 0.5 mL min^{-1}, 0.5% polysaccharide concentration and 0.1 M $NaNO_3$ as solvent, under the 30 °C of column temperature. A series of dextran standard with molecular weights ranging from 1250 to 5,70,000 were employed to generate the universal calibration curves for GGBr-g-AAP.

XRD analysis: The X-ray powder diffraction (XRD) patterns of guar gum and guar gum-g-(4-aminoantipyrine) were recorded on an X-ray diffraction SEIFERT RICH. SEIFERT and Co. Gmbh and Co. KG D-2070 Ahrensburg using Cu Kα as the radiation source (λ = 1.5418 Å) by varying the scattering angle (2θ) from 10 to 60°.

Thermal analysis: The thermal behaviour of guar gum and guar gum-g-AAP were recorded on SETARAM labsys thermal analyzer within a temperature range 80–800 °C in Argon atmosphere at heating rate of 10 °C/min. Differential scanning calorimetry (DSC) thermograms were recorded on Mettler Toledo TC 15 TA with the rate of 10.0 K min^{-1} under nitrogen atmosphere using spec pure grade indium as standard by taking samples in a sealed aluminium pans. Experiments were run under nitrogen in heat–cool–heat mode from +30 to +300 °C at heating and cooling rates of 10 °C/min. The glass transition temperatures from DSC were determined with accuracy of ±0.1 K.

The following parameters were calculated:

Grafting characteristics were obtained according to Fanta's definition (Fanta, 1973) (Eqs. (1)–(3)) in terms of grafting ratio (%*G*), grafting conversion (%*C*) and Add on (%*A*).

$$\%G = \frac{\text{weight of graft copolymer}}{\text{weight of GGBr}} \times 100 \quad (1)$$

$$\%A = \frac{\text{weight of synthetic polymer}}{\text{weight of graft copolymer}} \times 100 \quad (2)$$

$$\%C = \frac{\text{weight of polymer formed}}{\text{weight of monomer in feed}} \times 100 \quad (3)$$

where, graft copolymer = weight of guar gum-g-poly (4-aminoantipyrine), synthetic polymer = weight of graft copolymer − weight of guar gum macroinitiator

$$\text{Mn(Theo)} = \frac{\text{initial molar concentration of AAP}}{\text{initail average molar concentration of GGBr}} \times \text{conversion}_{\text{AAP}} \times M_{\text{AAP}} + M_{\text{GGBr}} \quad (4)$$

$$\text{DPn} = \frac{[\text{AAP}]_0}{[\text{GGBr}]_0} \times \text{conversion} \quad (5)$$

where, AAP = 4-aminoantipyrine monomer, GGBr = guar gum macroinitiator, M_{AAP} = molecular weight of monomer, Mn_{GGBr} = number average molecular weight of Guargum macroinitiator, $[AAP]_0$ = initial molar concentration of 4-amnioantipyrine monomer, $[GGBr]_0$ = initial average molar concentration of guar gum macroinitiator

Integral procedural decomposition temperature:

The integral procedural decomposition temperature (IPDT) which accounts the whole shape of the curve and it sum up all of its dips and meanderings in a single number by measuring the area under the curve. Thus thermal stability of pure guar gum and its graft copolymers has been determined by calculating IPDT values using following equation (Doyle, 1961). The area under the curve divided by the total area of graph is the total curve area, A^*, normalized with respect to both residual mass and temperature. A^* is converted to a temperature, TA^*, by following equation.

$$\text{TA}^* = (T_{\text{end}} - T_{\text{initial}})A^* + T_{\text{initial}} \quad (6)$$

TA^* represents a characteristic end of volatilization temperature rather than an IPDT having practical significance. The second curve area K^* can be derived by drawing rectangle bearing *X*-axis up to TA^* and the *Y*-axis mass fraction remaining at T_{end}. K^* is the ratio between the area under the curve (inside the rectangle) and total rectangle area. The IPDT determined by substituting A^*K^* for A^* in Eq. (6).

2.3. Synthesis of guar gum macro initiator

A 6% (w/v) solution of lithium chloride (LiCl) in dimethyl sulfoxide (DMSO) was prepared by heating 3 g of LiCl in 50 mL of anhydrous DMSO up to 150 °C in a 3-necked round bottom flask fitted with an overhead stirrer. Once a homogeneous solution was

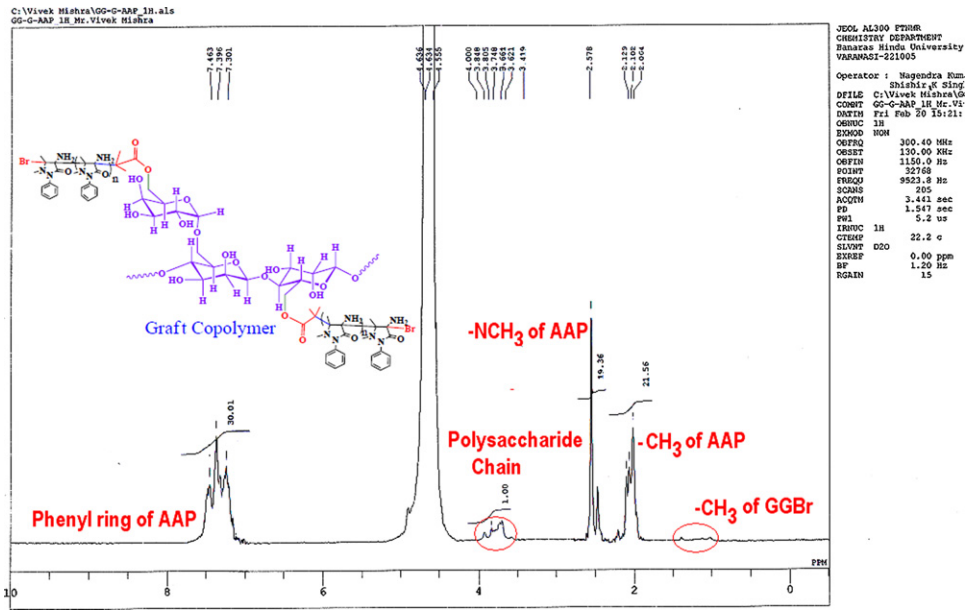

Fig. 1. ^{1}H NMR Spectra of GGBr-g-Poly (AAP) in D_2O.

obtained, 3 g guar gum was added to the solution gradually, maintaining the temperature at 150 °C until a highly viscous, clear, yellow solution was formed. The solution was cooled to 65 °C. In a separate beaker, a solution of 2-bromoisobutyric acid (4.5 g) in DMSO (50 mL) was prepared. To this solution, a solution of 1,1′-carbonyldiimidazole (4.5 g) in anhydrous DMSO (50 mL) was added slowly. Evolution of CO_2 gas indicates the formation of the imidazolide intermediate. Once the evolution of CO_2 has ceased, solution was added to the GG/DMSO/LiCl mixture with continuous stirring. The reaction was maintained at 65 °C for 24 h before pouring into a three-fold volume of methanol, causing the product to precipitate. The product was collected on a sinter funnel, redispersed into methanol, filtered and washed with three folds of methanol before being subjected to soxhlet extraction (methanol) for 48 h and dried in vacuum at 50 °C for a further 48 h, yielding 2.64 g of a creamy green coloured, solid. (Mn_{GPC} = 260,500): ^{1}H NMR (300 MHz; D_2O): δ 1.74 (d, 6H, H is $(CH_3)_2$C–Br), 1.98–2.12 (d), 2.62 (s, 6H, CH_3–DMSO), 3.41–4.64 (m, 25H, H on mannose/galactose ring of GG), 4.78 (d, 1H, anomeric H), 5.1 (d, 1H, anomeric H) (Fig. S3). FTIR (ν_{max}/cm^{-1}): 3426 (br, OH), 2926 (s, CH_2), 2852 (s, CH_3), 2078, 1739 (s, C=O ester), 1628 (s, C=O) (Fig. S6). UV (nm): 240–290 nm broad stretched shoulder (Fig. S8).

2.4. ATRP graft copolymerization of 4-aminoantipyrine with guar gum macroinitiator

The 0.01 g guar gum-macroinitiator was weighed and transferred into a 3-neck 100 mL round bottom flask filled with the 30 mL of distilled water to give a solid content of 3.3%. Flask was fitted with a N_2 inlet, thermometer, rubber septum and a syringe needle. This solution was left overnight in purified nitrogen atmosphere at room temperature to ensure complete dissolution of the macroinitiator. A reaction mixture of 1.0 g of 4-aminoantipyrine monomer, 0.02 g of 2,2′-bipyridyl and 0.01 g of Cu (I) Br was prepared in a 15 mL of water in another three neck flask; both the solutions (macro initiator and reaction mixture) were purged with purified nitrogen gas for 45 min at 10 °C prior to initiate the reaction. Further, to initiate the graft copolymerization, the solution of reaction mixture was transferred into the solution of macroinitiator by syringe keeping the temperature of the solution below 5 °C. Now reaction mixture was divided equally into nine Schlenk tubes. All Schlenk tubes were kept under same reaction condition. At the desired time polymerization was stopped by keeping the flask in liquid nitrogen (LNT) followed by opening the mouth and inlet of the flask. After 5–6 min reaction flask was taken out from the LNT flask. The content of the reaction flask was diluted with distilled water and the solution passed through a sintered glass funnel containing activated basic aluminium oxide attached to a Buchner flask. The filtrate was added to a 3-fold volume of methanol, causing the product to precipitate. The polymer was collected on a Petridish and dried in vacuum at 40 °C up to constant weight. Molar mass distribution was evaluated by GPC (Mn_{GPC} = 375,500). ^{1}H NMR δ (300 MHz; D_2O): 1.05–1.42 (t, 6H, H is $(CH_3)_2$C–Br), 2.004–2.129 (t, –CH_3 of monomer repeating unit), 2.578 (s/d, –NCH_3 of monomer repeating unit), 3.621–4.000 (m, H on mannose/galactose ring of GG), 7.301–7.463 (t, proton of phenyl ring of repeating 4-amino antipyrine) (Fig. 1). FTIR (ν_{max}/cm^{-1}): 3430, 3325, 2913, 1720, 1648, 1591, 1494, 1450, 1353, 1275, 1115, 758, 669, 572, 498 (Fig. S7). UV (nm): 298 and 309 (Fig. S8).

3. Results and discussion

3.1. Discussion on synthesis

The terminal bromide containing macroinitiator (GGBr) was prepared at 65 °C in DMSO using Guargum (GG), 2-bromoisobutyric acid and LiCl (Scheme 1). On comparing the ^{1}H NMR spectra of guargum (Fig. S2) and GGBr macroinitiator (Fig. S3), The presence of a doublet for methyl protons at 1.74 ppm ($(CH_3)_2$C–Br), a multiplet for protons of mannose/galactose ring of guargum at 3.41–4.64 ppm and a singlet for anomeric protons of mannose/galactose ring of guargum at 4.78 ppm (Fig. S3) in the product confirm the formation of macro initiator. On comparing the FTIR spectra of guargum (Fig. S5) and GGBr macroinitiator (Fig. S6), an extra absorption band at 1739 cm^{-1} in GGBr macroinitiator represents the appearance of carbonyl peak of α-keto ester group and 3426 cm^{-1} is due to unesterified –OH hydrogen bonded stretching vibration confirms the formation of the guar gum macroinitiator.

The synthesis of guar gum-g-poly (4-aminoantipyrine) was confirmed by ^{1}H NMR analysis. The appearance of a small hump shows the protons of $(CH_3)_2$C–Br at 1.05–1.42 ppm, triplet for repeating protons of –CH_3 of monomer unit at 2.004–2.129 ppm, singlet

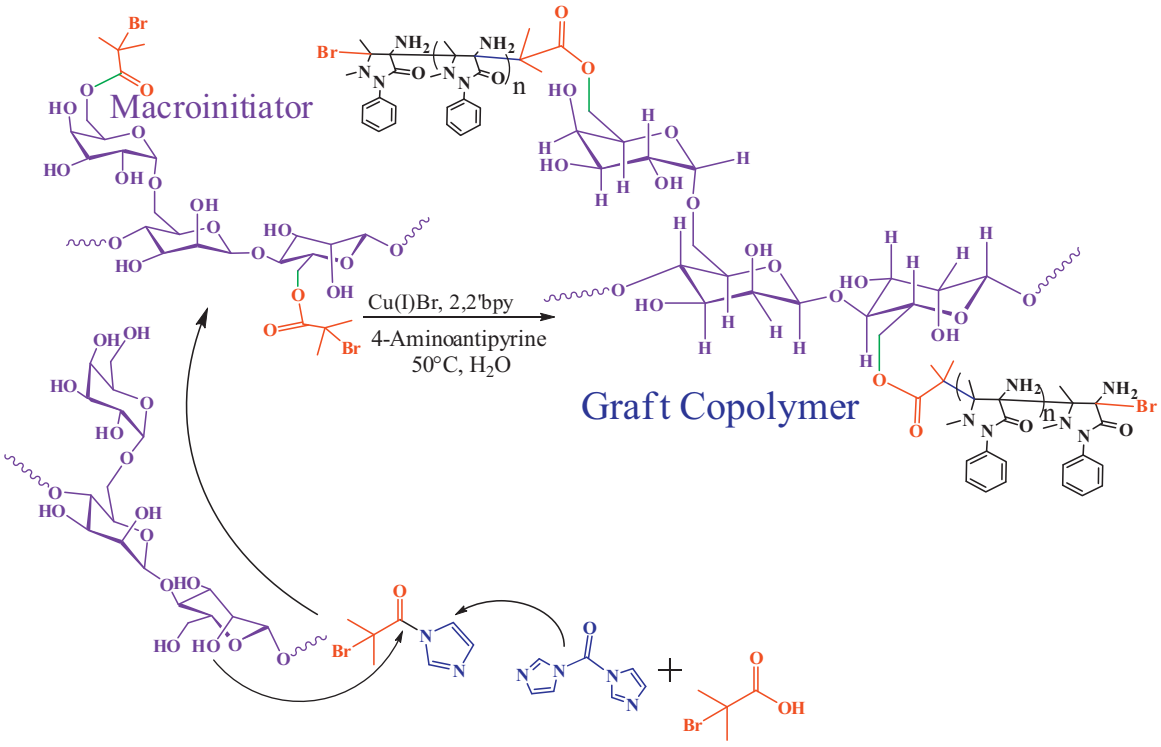

Scheme 1. Graft copolymerization of 4-aminoantipyrine from guar gum.

for repeating protons of $-NCH_3$ of monomer unit at 2.578 ppm, multiplet for protons of mannose/galactose ring of guar gum at 3.621–4.000 ppm and triplet for proton of repeating phenyl ring at 7.301–7.463 ppm supports the formation of guar gum grafted 4-aminoantipyrine polymer by ATRP method (Fig. 1). FTIR spectrum (Fig. S7) shows the peak at 3430 cm^{-1} appeared in guar gum-g-4-aminoantipyrine (GGBr-g-AAP), indicating the N–H stretching of amino group of 4-aminoantipyrine. The peak at 3325 cm^{-1} is due to the unesterified and non hydrogen bonded free hydroxyl group of guar gum substrate. The graft copolymerization is further confirmed by merged absorption of amide-I (>C=O stretching) at 1648 cm^{-1} and phenyl ring stretching at 1591 cm^{-1}. The bands at 1494, 1450, 1353 and 1275 cm^{-1} appear due to amide-II band, O–H bending, C–N stretching and interaction between C–N stretching and N–H bending, respectively. The appearance of these additional peaks in the spectrum shows the formation of the graft copolymer.

UV spectrum of 4-aminoantipyrine (Fig. S8) show two broad shoulders at 244 nm and 271 nm, which is due to the pyrazolone ring and electron transfer band of amino group of 4-aminoantipyrine. The spectrum for guar gum shows (Fig. S8) a small shoulder at 264 nm may be due to impurities in guar gum substrate, because polysaccharides are generally not expected to absorb here. A stretched broad shoulder was observed in guar gum initiator spectrum (Fig. S8) from 255 to 285 nm, which is due to the merging of n–π^* and π–π^* transition of the carbonyl group present in the macroinitiator. The UV spectrum of GGBr-g-AAP (Fig. S8) clearly indicates the incorporation of the above shoulders with a minor shift of 264–263 nm, and major shift in shoulder of 244 nm and 271 nm of 4-aminoantipyrine to 299 nm and 310 nm in the graft copolymer. The shifting in shoulders is due to structural alteration after polymerization, particularly the disappearance of conjugated double bonds in 4-aminoantipyrine.

Fig. 2 and Table 1 show a linear increase in conversion of 4-aminoantipyrine with time at a standard reaction condition. The correlation of $\ln[M]_0/[M]_t$ *w. r. t.* time is extremely good with an $r^2 = 0.998$, showing the absence of termination reactions and a steady concentration of propagating radicals throughout the polymerization. This is possibly due to more efficient initial radical production, leading to not only a higher concentration of active species but also an apparent control of the polymerization (Fig. 2). Fig. 3 shows that the $Mn_{(GPC)}$ increases from 361,400 to 375,500 while, molar mass distribution(Đm) decreases from 1.45 to 1.24 up to 23% conversion only, thereafter, slight increase in Đm was observed. The decrease in Đm and increase in $Mn_{(GPC)}$ and conversion shows the controlled linear growth of the graft copolymer up to 51% conversion at 12 h.

3.2. Determination of optimum reaction condition

3.2.1. Effect of 4-aminoantipyrine concentration

The effect of concentration of 4-aminoantipyrine on grafting parameters, molecular weight, degree of polymerization, molar mass distribution and initiator efficiency was investigated by varying the concentration of 4-aminoantipyrine from 0.5 to 1.5 g dm^{-3} (Table S1). It has been observed that % conversion, degree of poly-

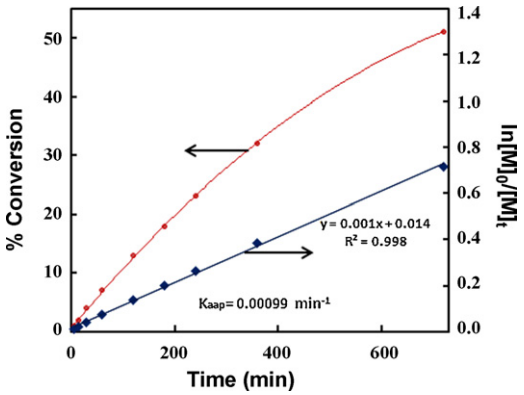

Fig. 2. Plot of time vs. monomer conversion and $\ln[M]_0/[M]_t$.

Table 1
Experimental conditions for GGBr-g-Poly(AAP) prepared by normal ATRP using GGBr as initiator[a].

Run	Time (in min)	$\ln[M_0/M_t]$	Mn_{theo}	Mn_{SEC}	Đm	% *C*	$\%G^c$	$\%G_{NMR}$[b]	$\%A^d$
1	5	0.01005	260,203	361,400	1.45	1	102	101	51
2	15	0.02020	260,406	361,600	1.42	2	203	194	67
3	30	0.04082	260,812	362,200	1.38	4	406	375	80
4	60	0.07257	261,421	363,000	1.34	7	711	656	88
5	120	0.13926	262,639	364,900	1.31	13	1322	1221	93
6	180	0.19845	263,654	365,800	1.26	18	1829	1732	95
7	240	0.26136	264,669	367,400	1.24	23	2338	2156	96
8	360	0.38566	266,496	369,600	1.25	32	3248	3012	97
9	720	0.71335	270,353	375,500	1.28	51	5184	4936	98

[a] [GGBr] = 0.01 g dm^{-3}, [AAP] = 1.0 g dm^{-3}, [Cu(I)Br] = 0.01 g dm^{-3}, [bpy] = 0.02 g dm^{-3}, AAP: water = 1/1 Time = 720 min. {$Mn_{guar\ gum}$(GPC) = 219,200, Mn_{GGBr}(GPC) = 260,500 found experimentally}.
[b] % Grafting through NMR is calculated by Wang & Wang (2010).
[c] ,[d]Calculated by Fanta's definition.

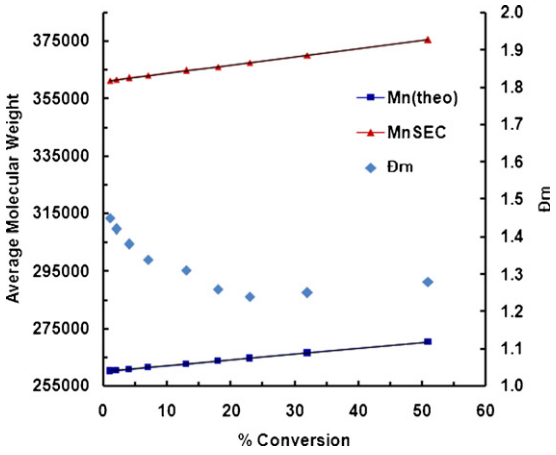

Fig. 3. Plot of AAP polymerization among M_n through theoretically, GPC and molar mass distribution of GGBr-g-Poly(AAP) as a function of AAP monomer conversion in water at 50 °C in the presence of $[Cu(I)Br]_o$:$[GGBr]_o$:$[bpy]_o$ = 1:1:2.

merization, grafting ratio and percent addon increase, respectively, on increasing the concentration of monomer. Table S1 (run 1–3) and Fig. 4 reveals that on varying the concentration of AAP from 0.5 to 1.5 g dm^{-3}, the number average molecular weight increases from 359,700 to 414,100, molar mass distributions from 1.26 to 1.56, respectively. This behaviour is attributed to accumulation of monomer molecules in close proximity of guar gum macroradical. The monomer molecules, which are at the immediate vicinity of reaction sites, become acceptors of guar gum macroradicals resulting in chain initiation and thereafter themselves

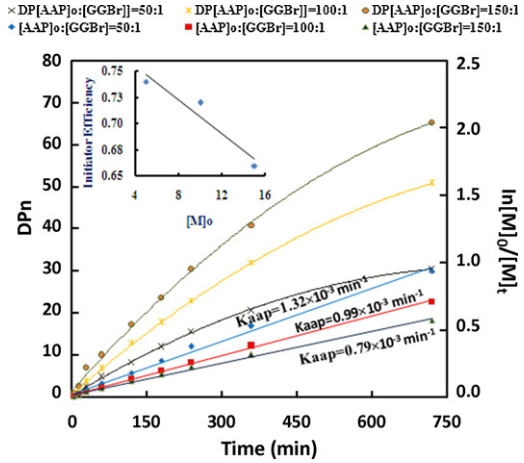

Fig. 4. Effect of monomer concentration on conversion and DP_n.

become free radical donors to the neighbouring monomer causing increase in the above parameters. An increase in degree of polymerizations from 31 to 65 is due to the increase in fraction of conversion of monomer into polymer (Eq. (3)). The initiator efficiency decreases from 0.74 to 0.66 and apparent rate constant from 1.32×10^{-3} min^{-1} to 0.79×10^{-3} min^{-1} (Fig. 4). This shows that concentration of monomer affects not only on the rate of polymerization but also the initiator efficiency. This is due to the diffusion limitations experienced by radical species and/or capping agents are one of the major factors for decreasing the efficiency of radical of guar gum macro initiator.

3.2.2. Effect of guar gum macroinitiator concentration

The effect of concentration of guar gum macroinitiator was observed with an aim of study the effect of its concentration (from 0.005 to 0.0015 g dm^{-3}) on grafting parameters, molecular weight, degree of polymerization, molar mass distribution and initiator efficiency in water at 50 °C for 12 h. Run 1, 4 and 5 of Table S1 and Fig. S10 reveals that the number average molecular weight (Mn_{GPC}) from 375,400 to 397,000; and molar mass distribution (Đm) from 1.22 to 1.56 increased, while conversion and initiator efficiency decrease from 53% to 44.2% and 0.75–0.67, respectively. This is due to the increase in the viscosity of reaction medium, which hinders the movement of free radicals that shifts the ATRP equilibrium towards Cu(II) species, which in turn produces excess radical, that shows the little uncontrolled graft copolymerization of AAP (Scheme 2).

3.2.3. Effect of Cu(I)Br/bipyridyl concentration ratio

The effect of catalyst/ligand ratio on grafting parameters, molecular weight, degree of polymerization, molar mass distribution and initiator efficiency was studied by varying the concentration ratio from 1:1 to 1:3 (Table S1 Run 1, 9 and 10). It was observed that grafting ratio, percent addon, and initiator efficiency increases from 3959 to 5589, from 97.54 to 98.24, from 0.71 to 0.75, respectively, on increasing the concentration of ligand. The increase in these parameters is attributed to the increase in number of primary free radicals with increase in bpy ligand concentration. Decrease in CuBr/ligand ratio from 1:1 to 1:3 ratio, Mn_{GPC} decreases from 377,400 to 361,600 but $Mn_{(Theo)}$ increases continuously. This deviation is due to (i) the relatively decrease in the concentration of propagating radical species with increase in conversion, (ii) the loss of considerable chain transfer reaction to monomer or highly reactive initiators are producing too many radicals, which are terminating at an earlier stage (Sha et al., 2006)

3.2.4. Effect of temperature

To find out the suitable temperature for living radical graft copolymerization of guar gum in aqueous medium, four set of experiments was carried out at different temperatures from 40 °C

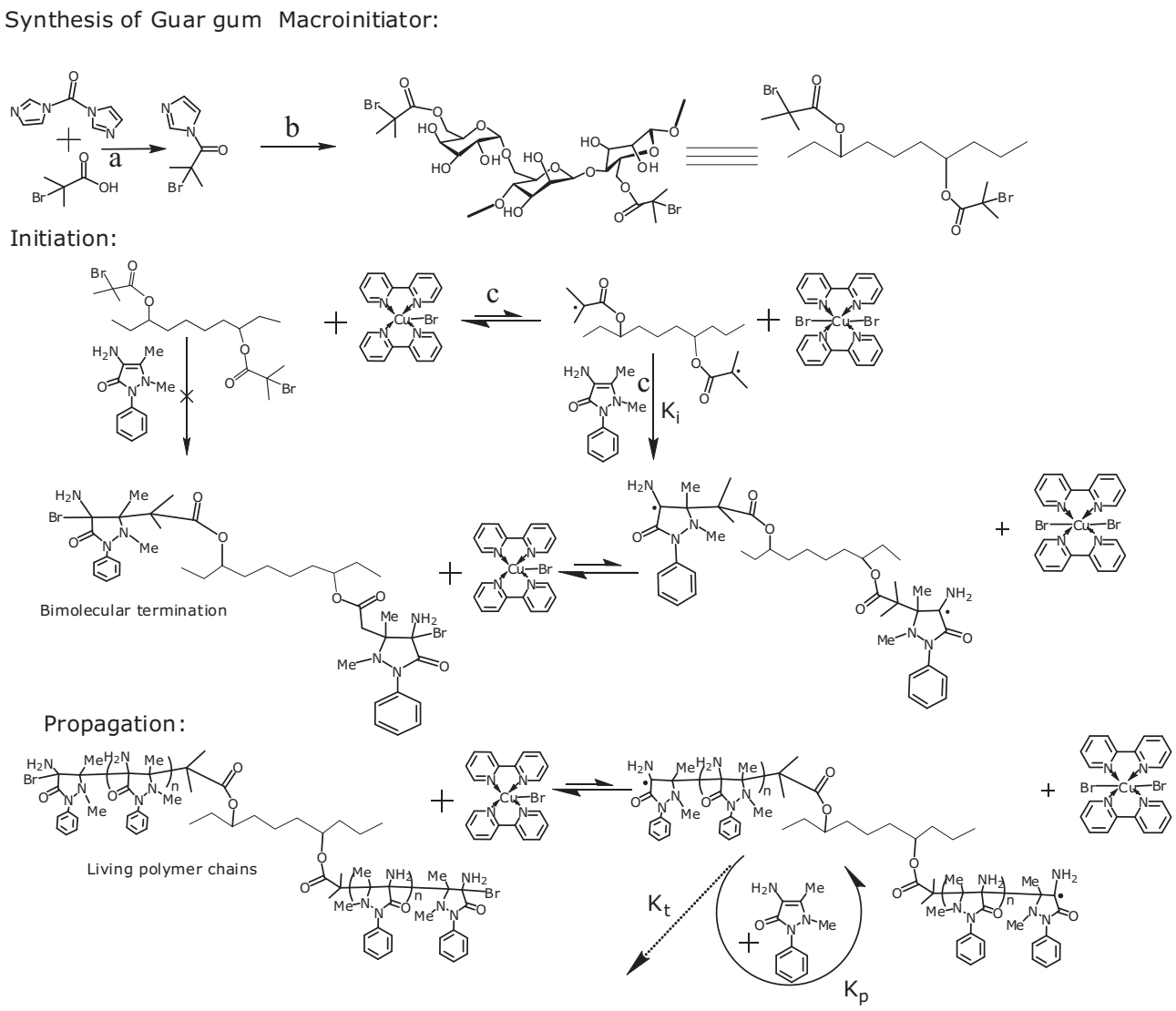

Scheme 2. Proposed mechanism of atom transfer radical graft copolymerization of AAP using Cu(I)Br/bpy catalytic system: a) LiCl, DMSO, 2-bromoisobutyric acid, CDI, 150 °C; b) 65 °C, Guar gum, DMSO, 24 h; c) 50 °C, H_2O, 4-aminoantipyrine in N_2 atmosphere.

to 70 °C; among them 50 °C was found best reaction temperature for graft copolymerization. As shown in run 1, 6–8 of Table S1, the % conversion increases from 40 to 69 with increase in temperature from 40 °C to 70 °C. Thus, when the reaction was performed at 40 °C (run 6 of Table S1), 40% conversion was observed in 12 h with 1.44 molar mass distribution. In same time at 50 °C (run 1 of Table S1), 51% conversion with 1.28 molar mass distribution, at 60 °C (run 7 of Table S1), 62% conversion with 1.46 molar mass distribution and at 70 °C (run 8 of Table 2), 69% conversion with 1.45 molar mass distribution were found. Therefore, graft copolymerization at 50 °C is more favourable due to good conversion with narrow molar mass distribution (Fig. 5). Fig. 5 also shows that the apparent rate of polymerization increases with increasing temperature due to increase of both the radical propagation rate constant and the atom transfer equilibrium constant (Sha et al., 2006). It has been observed that grafting ratio and percentage addon increase from 4060 to 7011 and 97.60–98.59, respectively, on increasing the temperature from 40 °C to 70 °C due to the increase in production of primary free radicals.

The temperature dependency of the apparent rate constants (k_{AAP}), the magnitudes of the activation enthalpy ($\Delta H^{\ddagger}$), activation entropy ($\Delta S^{\ddagger}$) and activation energy (E_a) were determined by evaluation of the linear Eyring and Arrhenius correlations (Fig. 5). The negative entropy ($\Delta S^{\ddagger} = -233.82\ J\ mol^{-1}\ K^{-1}$) is due to the sterically less demanding bromide moiety and greater flexibility of the activated complex. The negative value of $\Delta S^{\ddagger}$ suggests that at the transition state movement of reactants is highly restricted (Seeliger & Matyjaszewski, 2009), which supports the progress of reaction with time. The activation energy E_a (25.15 kJ mol^{-1}) and

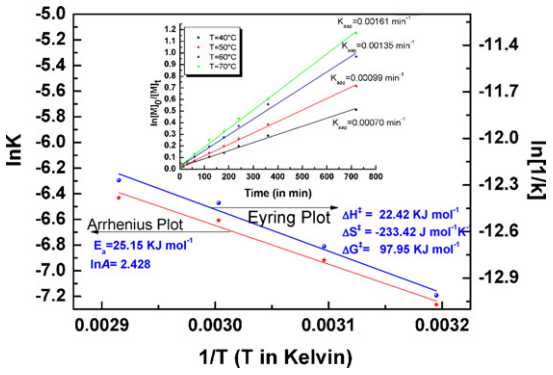

Fig. 5. Eyring and Arrhenius plot *w. r. t.* rate constants vs. 1/*T*. (In inset) Effect of Temperature on initial concentration of monomer at time.

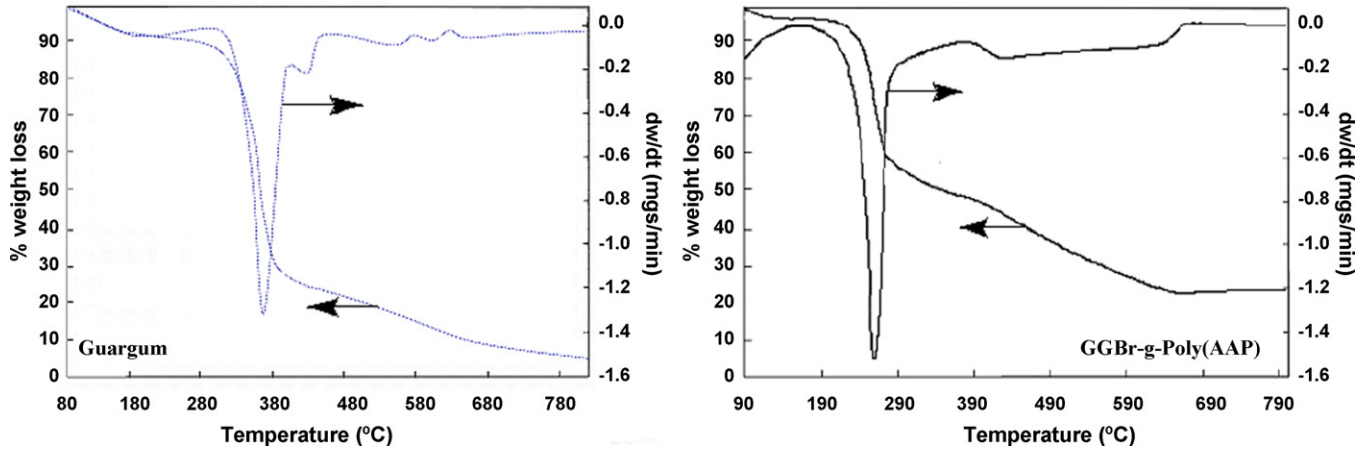

Fig. 6. TGA Chromatograms of guar gum and GGBr-g-Poly(AAP).

$\Delta H^{\ddagger}$ (22.42 kJ mol^{-1}) (Table S2) were very close to each other suggesting the feasibility of the reaction.

3.3. XRD analysis of GG-graft-copolymers

X-ray diffractograms of GG and GGBr-g-AAP samples are shown in Fig. S11. As clear from the above figure, none show any considerable peak for crystallinity. These results indicate that more branched structure is formed during radiation grafting, which restricts any long- or short-range orderliness in the samples, hence, the samples are amorphous to a great extent and no significant peak for crystallinity is observed for these samples.

3.4. TGA analysis of GG-graft-copolymers

3.4.1. Guar gum

Fig. 6 shows the thermogram of guar gum which reveals that the decomposition of guar gum started at 230 °C and predominantly it is single step degradation from 200 to 314 °C, while three small degradation steps have also been observed from 370 °C to 564 °C. The rate of weight loss increased on increasing temperature up to 310 °C, but thereafter, rate of weight loss was decreased. About 60% weight loss was occurred between 200 and 314 °C and it is due to polysaccharide decomposition and this leads to the separation of galactose and mannose units taken place from polysaccharides (Varma, Kokane, Pathak, & Pradhan, 1997; Vendruscolo et al., 2009). These two units further degrades gradually at 370 °C with the loss of about 66% total weight, 508 °C (77%), 564 °C (88%) total weight loss were observed. Nearly 75% of guar gum degraded at 400 °C and about 5% char yield was obtained at 800 °C. Therefore the final decomposition temperature (FDT) was found at very low temperature i.e., 320 °C. IPDT values was found to be 318.8 °C, calculation shows the T*A** at 415 °C which gives the end of volatilization of guar gum.

3.4.2. Guar gum-g-AAP

Guar gum-g-AAP (Fig. 6) starts degrade at about 200 °C. The rate of weight loss increased on increasing the temperature from 150 °C to 400 °C, but thereafter it decreases slowly (Fig. 6). About 48% weight loss was observed at 400 °C, while 50% weight loss in case of guar gum was observed at 310 °C and a char yield of 26% was obtained at 800 °C (Tables S4 and S5). The maximum weight loss (T_{max}) appeared at 260 °C which is due to poly(4-aminoantipyrine) degradation in the temperature range of 175–300 °C by the formation of imide group via cyclization of imide group and evolution of ammonia (Fig. 6). This cyclized structure imparts further stability to guar gum molecule. PDT, FDT, IPDT of guar gum-g-AAP were found to be 238 °C, 626 °C and 317.3 °C, respectively (Table S3). The value of PDT and FDT indicated that grafting of 4-aminoantipyrine decreases the initial decomposition temperature by 22 °C while it increases the final decomposition temperature to 306 °C. The grafting of 4-aminoantipyrine lowers the initial decomposition temperature of graft copolymers. The higher value of FDT, IPDT and char yield of grafted guar gum compared to those of guar gum indicates an overall improvement in thermal stability of the graft copolymer.

3.5. DSC analysis of guar gum and guar gum-g-AAP

A second thermal study was made by DSC in order to estimate the influence of the monomer on the guar gum (Fig. S12A). The measured T_g of guar gum is higher than the grafted guar gum from 4-aminoantipyrine (Fig. S12B). This is might be due to the 4-aminoantipyrine pendent chains become more flexible in movement leading the grafted guar gum to be more flexible than pure guar gum, so guar gum segment need less energy to pass from a glassy state to rubbery state thereby decreasing its glass transition temperature (Laruelle, Parvole, Francois, & Billon, 2004).

3.6. Reaction mechanism

The unique step in ATRP involves the dynamic equilibrium between active and dormant polymer chains. A low oxidation-state metal halide Cu (I) Br complexed with ligand undergoes one-electron oxidation and abstracts the halogen atoms from the GGBr macroradical, producing $CuBr_2$ to generate two tertiary radicals on GGBr, which further transfer the electron to the monomer which ultimately generates graft copolymer radical. The radical activation and metal oxidation reactions are reversible. The abstracted halogen atom can easily go back to cap a polymer radical, which further propagated as shown in Scheme 2.

4. Conclusion

ATRP graft copolymerization of 4-aminoantipyrine was successfully carried out using “grafting from” methodology in an eco-friendly environment (aqueous medium) at ambient temperature. The negative entropy ($\Delta S^{\ddagger} \approx -233.82$ J mol^{-1} K^{-1}), activation energy E_a (25.15 kJ mol^{-1}) and $\Delta H^{\ddagger}$ (22.42 kJ mol^{-1}) shows the progress of the reaction. Pseudo-first order kinetics was observed and a polydispersibility as low as 1.28 was obtained. High percentage of grafting is achieved without the formation of homopolymer.

The graft copolymer is thermally more stable, but has a lower T_g than unmodified guar gum.

Acknowledgements

The authors thank to the Head, Department of Chemistry, BHU, Varanasi (India) for providing spectral and analytical facilities and thanks are due to Department of Ceramic Engineering, IT BHU, Varanasi for providing TGA thermograms and XRD pattern. Financial assistance in the form of Fast Track Project (SR/FTP/CS-107/2005) from DST New Delhi is gratefully acknowledged. Finally yet importantly, the authors are thankful to the reviewers for their useful comments and clarifying our understanding on our observation.

Appendix A. Supplementary data

Supplementary data associated with this article can be found, in the online version, at doi:10.1016/j.carbpol.2011.04.052.

References

Banerjee, J., Kumar, R., Srivastava, A., & Behari, K. (2006). Graft copolymerization of 2-acrylamido-2-methyl-1-propanesulphonic acid onto carboxymethylcellulose (sodium salt) using bromate/thiourea redox pair. *Journal of Applied Polymer Science*, *100*, 26.

Beers, K. L., Gaynor, S. G., Matyjaszewski, K., Sheiko, S. S., & Moeller, M. (1998). The synthesis of densely grafted copolymers by atom transfer radical polymerization. *Macromolecules*, *31*, 9413.

Behari, K., Kumar, R., Tripathi, M., & Pandey, P. K. (2001). Graft copolymerization of methacrylamide onto guar gum using potassium chromate/malonic acid redox pair. *Macromolecular Chemistry and Physics*, *202*, 837.

Behari, K., Pandey, P. K., Kumar, R., & Taunk, K. (2001). Graft copolymerization of acrylamide onto xanthan gum using Fe^{2+}/BrO_3^- redox couple. *Carbohydrate Polymers*, *46*, 185.

Desai, B., Modi, S., & Naik, H. B. (1994). Studies on pyrazolines-Part-I: preparation and antibacterial activity of 1-H-3-(2′-hydroxy-4′-n-propoxyphen-1′-yl)-5-substituted phenyl-2-pyrazolines. *Journal of Indian Council of Chemists*, *10*, 1.

Doyle, C. D. (1961). Estimating thermal stability of experimental polymers by empirical thermo gravimetric analysis. *Analytical Chemistry*, *33*, 77.

Ebouc, F., Dez, I., Desbrieres, J., Picton, L., & Madec, P.-J. (2005). Different ways for grafting ester derivatives of poly(ethylene glycol) onto chitosan: related characteristics and potential properties. *Polymer*, *46*, 639.

Fanta, G. F. (1973). Properties and applications of graft and block copolymers of starch. In R. J. Ceresa (Ed.), *Block and Graft Copolymerization*. New York, NY, London, England: Wiley-Interscience, pp. 29

Gorochovceva, N., & Makuska, R. (2004). Synthesis and study of water-soluble chitosan-O-poly (ethylene glycol) graft copolymers. *European Polymer Journal*, *40*, 685.

Huang, M., Shen, W., & Fang, Y. (2005). Synthesis of a novel chitosan derivative having poly(ethylene oxide) side chains in aqueous reaction media. *Reactive and Functional Polymers*, *65*, 301.

Jenkins, D. W., & Hudson, S. M. (2001). Review of vinyl graft copolymerization featuring recent advances toward controlled radical-based reactions and illustrated with chitin/chitosan trunk polymers. *Chemical Reviews*, *101*, 3245.

Kadu, M. V., & Jamode, V. S. (1998). Synthesis of 3,5-diaryl-4-benzoyl-1-pyridoyl-2-pyrazolines. *Asian Journal of Chemistry*, *10*, 367.

Kadu, M. V., Jamode, V. S., & Tambekar, D. H. (1999). Antibacterial activities of 3,5-diaryl-4-benzoyl-1-pyridoyl-2-pyrazolines. *Asian Journal of Chemistry*, *11*(3), 1064.

Kamigaito, M., Ando, T., & Sawamoto, M. (2001). Metal-catalyzed living radical polymerization. *Chemical Reviews*, *101*, 3689.

Kumar, R., Srivastava, A., & Behari, K. (2007). Graft copolymerization of methacrylic acid onto xanthan gum by Fe^{2+}/H_2O_2 redox initiator. *Journal of Applied Polymer Science*, *105*, 1922.

Kumar, R., Srivastava, A., & Behari, K. (2008). One-pot synthesis of a polysaccharide-based graft copolymer with an efficient redox pair (Fe^{2+}/BrO_3^-). *Journal of Applied Polymer Science*, *107*, 2883.

Kumar, R., Srivastava, A., & Behari, K. (2009). Synthesis and characterization of polysaccharide based graft copolymer by using potassium peroxymonosulphate/ascorbic acid as an efficient redox initiator in inert atmosphere. *Journal of Applied Polymer Science*, *112*, 1407.

Kurita, K., Amemiya, J., Mori, T., & Nishiyama, Y. (1999). Comb-shaped chitosan derivatives having oligo (ethylene glycol) side chains. *Polymer Bulletin*, *42*, 387.

Laruelle, G., Parvole, J., Francois, J., & Billon, L. (2004). Block copolymer grafted silica particles: a core/double shell hybrid inorganic/organic material. *Polymer*, *45*, 5013.

Matyjaszewski, K., & Xia, J. (2001). Atom transfer radical polymerization. *Chemical Reviews*, *101*, 2921.

Metwally, M. A., Yousif, M. Y., Ismaiel, A. M., & Amer, F. A. (1985). Syntheses of some arylsulfonylpyrazolines and pyrazolones as potential antipyretic analgesic agents. *Journal of the Indian Chemical Society*, *62*, 54.

Mishra, V., & Kumar, R. (2011). Synthesis and characterization of five-arms star polymer of N-vinyl pyrrolidone through ATRP based on Glucose. *Carbohydrate Polymers*, *83*, 1534–1540.

Raman, N., Kulandaisamy, A., Shunmugasundaram, A., & Jeyasubramanian, K. (2001). Synthesis, spectral, redox and antimicrobial activities of Schiff base complexes derived from 1-phenyl-2,3-dimethyl-4-aminopyrazol-5-one and acetoacetanilide. *Transition Metal Chemistry*, *26*, 131.

Roos, S. G., Muller, A. H. E., & Matyjaszewski, K. (2000). Copolymerization of n-butyl acrylate with methyl methacrylate and PMMA macromonomers by conventional and atom transfer radical copolymerization. In *ACS Symposium Series 768 (Controlled/Living Radical Polymerization)* (p. 361).

Sachchar, S. P., & Singh, A. K. (1985). Synthesis of some new fluorinated heteroaryl pyrazolines and isooxazolines as potential biocidal agents. *Journal of the Indian Chemical Society*, *62*, 142.

Samath, S. A., Jeyasubramanian, K., Thambidurai, S., Kamardeen, S., & Ramalingam, S. K. (1993). Reactions of coordinated-ketoesters A new route for the synthesis of 4-substituted-3-methyl/phenyl-1-phenyl pyrazol-5-ones via a metal chelated stable intermediate. *Polyhedron*, *12*, 1265.

Seeliger, F., & Matyjaszewski, K. (2009). Temperature Effect on Activation Rate Constants in ATRP: New Mechanistic Insights into the Activation Process. *Macromolecules*, *42*, 6050–6055. DOI: 10.1021/ma9010507.

Sha, K., Li, D., Li, Y., Ai, P., Wang, W., Xu, Y., et al. (2006). The chemoenzymatic synthesis of AB-type diblock copolymers from a novel bifunctional initiator. *Polymer*, *47*, 4292.

Shinoda, H., & Matyjaszewski, K. (2001). Structural control of poly (methyl methacrylate)-g-poly (lactic acid) graft copolymers by atom transfer radical polymerization (ATRP). *Macromolecules*, *34*, 6243.

Shinoda, H., Miller, P. J., & Matyjaszewski, K. (2001). Improving the structural control of graft copolymers by combining atrp with the macromonomer method. *Macromolecules*, *34*, 3186.

Srivastava, A., Mishra, V., Singh, S.K., & Kumar, R. (2009). One pot synthesis and characterization of industrially important graft copolymer (GOH-g-ACM) by using peroxymonosulphate/mercaptosuccinic acid redox pair. *e-Polymers*, No. 006, 1.

Srivastava, A., Mishra, V., Singh, S. K., & Kumar, R. (2010). Vanadium (V)/Mandelic acid initiated graft copolymerization of acrylamide onto guar gum in an aqueous medium. *Journal of Applied Polymer Science*, *115*, 2375, 10.1002/app.31172.

Tayde, V. B., & Jamode, V. S. (1998). Studies on the antibacterial activity of 3,5-diaryl pyrazolines and 3,5-diaryl pyrazoles. *Asian Journal of Chemistry*, *10*, 1023.

Tripathi, M., Behari, K., Taunk, K., & Kumar, R. (2000). Studies of graft copolymerization of acrylamide onto guar gum using peroxy diphosphate/metabisulphite redox pair. *Polymer International*, *49*, 153.

Utale, P. S., Raghuvanshi, P. B., & Doshi, A. G. (1998). Synthesis of some new 1-carbamoyl-3-(substituted 2-hydroxyphenyl)-5-aryl-2-pyrazolines. *Asian Journal of Chemistry*, *10*, 597.

Varma, A. J., Kokane, S. P., Pathak, G., & Pradhan, S. D. (1997). Thermal behavior of galactomannan guar gum and its periodate oxidation products. *Carbohydrate Polymers*, *32*, 111–114.

Vendruscolo, C. W., Ferrero, C., Pineda, E. A. G., Silveira, J. L. M., Freitas, R. A., Jiménez-Castellanos, M. R., et al. (2009). Physicochemical and mechanical characterization of galactomannan from Mimosa scabrella: Effect of drying method. *Carbohydrate Polymers*, *76*, 86–93.

Wang, J.-S., & Matyjaszewski, K. (1995). Controlled/"living" radical polymerization. Atom transfer radical polymerization in the presence of transition–metal complexes. *Journal of the American Chemical Society*, *117*, 5614.

Wang, Q., & Wang, Y. (2010). Synthesis of novel amphiphilic graft copolymers composed of poly(ethylene oxide) as backbone and polylactide as side chains. *Journal of Polymer Research*, *1–7*, 10.1007/s10965-010-9428-y.

Wang, X. S., Lascelles, S. F., Jackson, R. A., & Armes, S. P. (1999). Facile synthesis of well-defined water-soluble polymers via atom transfer radical polymerization (ATRP) in aqueous media at ambient temperature. *Chemical Communications*, 1817.